Journal of Experimental Nanoscience
Publication details, including instructions for authors and subscription information:
http://www.informaworld.com/smpp/title~content=t716100757

Fluidisation behaviour of silica nanoparticles under horizontal vibration

Wei Zhang[a]; Ming Zhao[a]
[a] E-max Petrochemical Co. Ltd, P.R. China

Online publication date: 08 February 2010

To cite this Article Zhang, Wei and Zhao, Ming(2010) 'Fluidisation behaviour of silica nanoparticles under horizontal vibration', Journal of Experimental Nanoscience, 5: 1, 69 — 82
To link to this Article: DOI: 10.1080/17458080903260944
URL: http://dx.doi.org/10.1080/17458080903260944

Journal of Experimental Nanoscience
Vol. 5, No. 1, February 2010, 69–82

Taylor & Francis
Taylor & Francis Group

Fluidisation behaviour of silica nanoparticles under horizontal vibration

Wei Zhang* and Ming Zhao

E-max Petrochemical Co., Ltd, Shenyang 110117, P.R. China

(*Received 8 October 2008; final version received 13 August 2009*)

In present study, fluidization behaviour of silica nanoparticles with primary size between 7 and 16nm under horizontal vibration was investigated. Fluidization characteristics were assessed by observing pressure drop, bed expansion and bed collapse behaviour at the vibration frequencies between 0 and 34 Hz. Horizontal vibration is demonstrated to be as effective as the vertical configuration reported previously in terms of fluidization improvement. In all cases, smooth agglomerate particulate fluidization was observed at vibrational frequencies greater than 16.7 Hz as long as the vibrational amplitude is set to be more than 1. This is much lower than previous reported value, and suggests that fluidization assisted with horizontal vibration is a promising technique for the large scale processing of nanomaterials (e.g. reacting, dispersing, or coating).

Keywords: agglomerates; nanoparticles; vibration; fluidisation; silica

1. Introduction

The gas–solid fluidisation technique has found its place in a variety of industrial applications because of the good capability of continuous processing, good solid–solid/gas–solid mixing and excellent heat and mass transfer. Depending on the process requirements, the particle size of the solid material ranges from several microns, e.g. catalytic cracking of hydrocarbons, up to several millimetres in a spouted bed, e.g. for the drying of wheat [1]. Solid particles exhibit distinctive fluidisation behaviours as a function of size and density. In the early 1970s, Geldart classified particles into four groups: Group A for aeratable particles, Group B for bubbling particles, Group C for cohesive particles and Group D for large spoutable particles [2]. Extensive research has been undertaken on the gas fluidisation of 'classical' particles in the size range of 30–1000 μm (falling under Geldart group A and B particles), and consequently, their fluidisation behaviour is well understood. Being able to process fine or ultrafine materials is advantageous because their small size and large-surface-area ratio allows good interparticle contact, and hence enhanced reaction efficiency. As a consequence, from the mid-1980s, research on the fluidisation behaviour of fine and ultrafine (nano–sized) particles has become more popular, predominantly in pharmaceutical and materials science applications, e.g. coatings, electronics, ceramics and catalysis [3–5]. In many of

*Corresponding author. Email: sytvzm2009@yahoo.cn

ISSN 1745–8080 print/ISSN 1745–8099 online

DOI: 10.1080/17458080903260944
http://www.informaworld.com

these applications, it is necessary to first disperse the nanoparticles, and indeed, fluidised beds are ideal for this task. However, the fluidisation of nanoparticles, which has more complex behaviour due to strong interparticle interactions (such as Van der Waals, electrostatic and moisture-induced surface tension forces), is more difficult to achieve. Under such conditions, the gas tends to flow through fixed paths, called stable channels. When stable channels are formed in the bed, both the efficiency of gas–solid contact and the fluidity of the bed are reduced. This has limited the large-scale processing of nanoparticle materials using fluidised beds related equipments.

To overcome this difficulty, some progress has been made in the literature. Several researchers successfully fluidised nanoparticles by employing various external force assistances, e.g. electromagnetic field, acoustic and mechanical agitation and centrifugal field [6]. Among those, mechanical vibration can significantly reduce the occurrence of channelling compared to that in the conventional fluidised beds [7–13]. Other advantages include reduced minimum fluidisation velocity and elutriation. Most of the works published thus far on the vibration-assisted fluidisation of nanoparticles were limited to the vertical configuration and higher frequencies between 30 and 200 Hz. As a consequence, the information on the full potential of vibrofluidisation (i.e. lower limit of frequency, vibration configurations) was insufficient to this end.

In this work, we report on the horizontal vibrofluidisation of three types of silica nanoparticles at frequencies between 0 and 34 Hz. The silica nanoparticles were chosen primarily because they have been used previously to investigate the fluidisation characteristic of nanoparticles, and hence there exists a body of work for comparison. This is particularly important for fluidisation studies, where much of the theory developed to explain the observed behaviour is empirical. Without a suitable body of experimental data from which design correlations can be derived, it is impossible to accurately design large-scale fluidisation equipments. The influences of different experimental variables, such as primary particle size, particle surface characteristics, vibration frequency and intensity, on the macroscopic fluidisation behaviour of nanoparticles were examined to clarify the effects of vibration on the fluidisation of nanoparticles. We envisage that this clarification will be useful in terms of obtaining suitable operational conditions for the large-scale nanoparticles processing with vibrofluidised beds.

2. Experimental details

2.1. *Equipment*

The layout of the experimental vibrofluidised bed system is illustrated in Figure 1. A fluidised bed was constructed from a glass column, which was able to minimise the influence of static electricity. The distributor is a porous glass frit with a nominal pore size range of 150–200 μm and located 5 cm from the bottom of the column. The chamber between the frit and the bottom of the column was filled with glass beads of approximately 2.5 mm diameter to ensure even gas distribution through the frit to the bed. This chamber is typically known as a plenum chamber or windbox in fluidised bed. The top of the column was connected, via flexible tubing, to a series of traps containing dilute solutions of potassium hydroxide, to ensure the capture of any elutriated nanoparticles prior to the fluidising gas being discharged to the laboratory extract system. The bed was fluidised with compressed air supplied at 90 psig and dried by passing through a calcium chloride

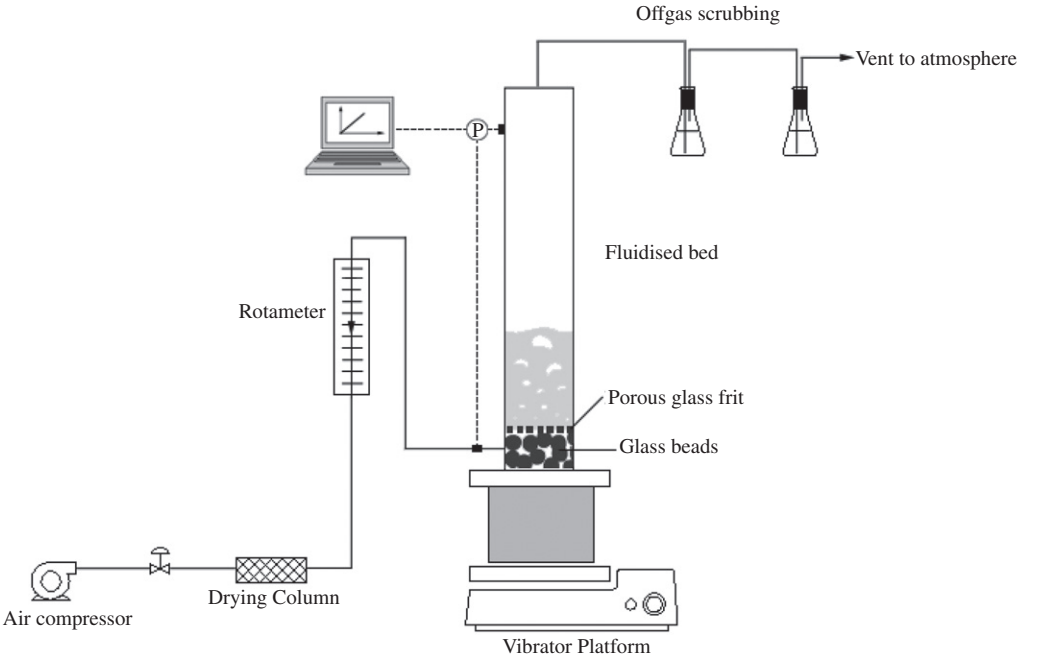

Figure 1. Schematic representation of the vibrofluidised bed system.

drying column. The flow rate of the fluidising air was measured using rotameters calibrated with a Minibuck® soap bubble column. All experiments were undertaken at ambient temperature. During each experiment, pressure was measured using a transducer located between the plenum chamber and the top of the bed, and the bed height was measured using a scale marked along the side of the column.

The entire apparatus was mounted on a vibrating platform (IKA Vibrax VXR) which supplied horizontal vibration frequencies between 1.67 and 33.67 Hz, at a stroke amplitude of 4 mm in the horizontal plane. In most previous studies for characterising the vibration intensity of vertical configurations, the vibration parameter, I, which is the ratio of the vibration acceleration to gravitational acceleration, was defined as follows:

$$I = \frac{A_0\omega^2}{g} \tag{1}$$

where A_0 (mm) is peak amplitude, ω is the angular frequency and $\omega = 2\pi fs^{-1}$. No numerical model of satisfactory precision has yet been obtained. Despite this, some vibrofluidisation behaviours (i.e. pressure drop, bed height and porosity) are found to be non-linear functions of I [14]. In this study, dimensionless values of I vary from 1.1 to 17.6.

2.2. *Particulate materials*

The particulate materials used in this work were fumed silica nanoparticles which are commercially available from Degussa AG. As a result of surface modification by the

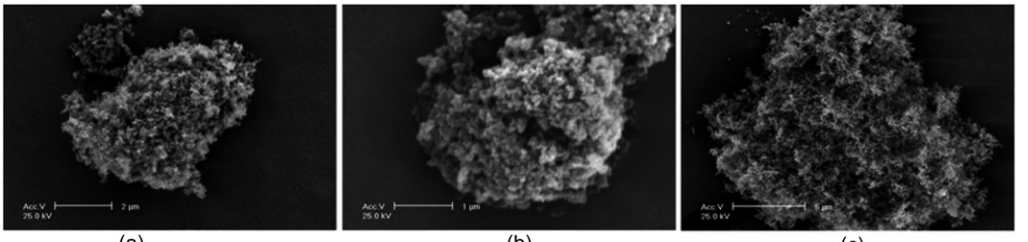

Figure 2. Scanning electron microscopy (SEM) images of the particles used in this work, as received from the supplier. These particles form large, light agglomerates to minimise the overall surface energy. (a) Aerosil R812; (b) Aerosil 300 and (c) Aerosil R972.

manufacturer R812 and R972 are strongly hydrophobic, whereas Aerosil 300 is hydrophilic. Scanning electron microscopy images of the 'as received' particles are shown in Figure 2. These images suggest that the particles form large, weak agglomerates during storage, which can be several millimetres in diameter. These are easily broken down into smaller agglomerates by mechanical agitation. All experimental variables are summarised in Table 1.

2.3. *Experimental procedures*

The fluidisation characteristics of the silica nanoparticles were inferred using bed expansion and bed collapse experiments. During a bed expansion experiment, the bed height and pressure drop across a particle bed are monitored as a function of superficial gas velocity through the bed. During a bed collapse experiment, the bed was allowed to reach a stable fluidised state and the change in the bed height was monitored with time for three types of bed collapse behaviour, (1) aeration on and vibration off, (2) aeration off and vibration on and (3) both of them off. These techniques have been used previously for assessing the fluidisation behaviour of solid particles, including nanosized particles.

Prior to all experiments the initial bed height was first adjusted to 50 mm, and then the bed was shaken by mechanical vibration at 34 Hz for 20 s before any aeration was turned on. Previously, without aeration, Valverde [15] found that vibrofluidised beds of cohesive particles exhibit two different regimes. In the solid-like regime, the bed will compact much like a bed of non-cohesive particles being vibrated into a settled state. It was found that if the vibration is then stopped, the bed does not expand back to its original height. In the fluid-like regime, the bed will expand until a critical vibration intensity is reached. At this point, bubbles form and cause sloshing at the top of the bed. If the vibration is then stopped, the bed expands back to its original height. Accordingly, the high-intensity vibration was chosen here to diminish the chances of very large agglomerates that may have been generated by storage or transportation, and simultaneously ensure a consistent starting point for each experiment, i.e. bed height.

During each experiment, the vibration frequency was set and then the fluidising air was supplied to the bed. During each experiment, the fluidising gas velocity was raised in steps of 0.005 m/s, from zero to the column maximum (the point at which the particle bed

Table 1. Vibrofluidised bed design parameters and experimental conditions.

	Value
Fluidisation column diameter (mm)	60
Fluidisation length (mm)	300
Vibrator frequency (Hz)	8.4, 16.8, 25, 33.4
Vibrator peak amplitude (mm)	4 mm
Vibration parameter, I	1.1, 4.5, 9.9, 17.6
Particulate material	(a) Aerosil R812 (b) Aerosil R972 (c) Aerosil 300
Average primary particle size (nm)	(a) 7 (b) 16 (c) 7
Bulk density (kg/m^3)	(a) 38.29 (b) 39.00 (c) 37.15
Particle density (kg/m^3)	(a) 2560 (b) 2560 (c) 2560
Typical BET surface area (m/g)	(a) 230–290 (b) 90–130 (c) 270–130
Surface modification	(a) Yes (b) Yes (c) Yes
Behaviour with water	(a) Hydrophobic (b) Hydrophobic (c) Hydrophilic

reached the top of the column), decreased to zero and then raised to the maximum again. The pressure drop and bed height as a function of fluidising velocity were recorded in each case. The results presented in Section 3 are the average of two sets of measurements at the same experimental conditions. Hysteresis curves were also measured for each experiment, i.e. the bed height was recorded with increasing gas flowrate (fluidisation) and then with decreasing gas flowrate (defluidisation). In traditional fluidised beds this is used to determine the location of the minimum fluidisation velocity (the point at which the bed first becomes 'fluidised'). Visual observations of the fluidisation behaviour and agglomeration tendency were recorded using a high-speed camera.

3. Results and discussion

3.1. *Fluidisation of silica nanoparticles without mechanical vibration*

Previously, Wang et al. [16] demonstrated smooth, agglomerating fluidisation, in the absence of any external force, using Aerosil 300, R812 and R972 particles, in a

glass column. On the basis of their experiments, Wang et al. defined two general types of fluidisation behaviour for nanoparticles:

(i) Very smooth fluidisation occurring with extremely high bed expansion and practically no bubbles, where the velocity as a function of voidage around the fluidised agglomerates obeyed the Richardson–Zaki equation. Wang et al. termed this agglomerate particulate fluidisation (APF); during APF, the expanded beds have a 'texture' that is closer to the fluidisation in a liquid–solid system than to the bubbling fluidisation in a gas–solid system.
(ii) Fluidisation within limited bed expansion and large bubbles rose very quickly through the bed. This type of fluidisation was termed agglomerate bubbling fluidisation (ABF).

Zhu et al. [17] later postulated that the transition between these regimes was primarily due to the physical properties of agglomerates, i.e. particle size and bulk density, rather than that of primary particles. They noted, however, that very little experimental data on the fluidisation characteristic and difference between APF and ABF exists in the literature.

Nevertheless, we were unable to reproduce the aforementioned observations in the present work. A typical result for Aerosil 300, in the absence of vibration, is illustrated in Figure 3. As the superficial gas velocity was increased from 0 to 0.18 m/s, four distinct types of behaviours were observed within the bed of particles.

(i) At low gas velocity (0.01–0.03 m/s), cracking and channelling occurred, beginning at the wall and eventually spreading to the centre of the bed. When the rate of increase in superficial gas velocity was high, e.g. >0.05 m/s, the whole bed of particles was lifted as single solid plug, and was ejected from the top of the column.
(ii) Between 0.03 and 0.07 m/s, the bed expanded to maximum height of 7 cm (from an initial height of 5 cm) and appeared to be 'coarsely' fluidised with large bubbles clearly observable.
(iii) At gas velocities above 0.07m/s, the bed height began to decrease, and large agglomerates were observed to form at the base of the bed adjacent to the distributor.
(iv) Eventually, the bed of particles reached a stable height of 5.5 cm. At this point, the bed comprised three distinct regions:

    (a) a packed bed of spherical agglomerates, roughly 2–3 mm in size, comprising $\sim$1/3 of the total bed height, and located adjacent to the distributor,
    (b) a region above this of smaller agglomerates that was slightly expanded and
    (c) a thin region of fine material above this that appeared to float above the layers of agglomerates.

This type of behaviour observed is shown conceptually in Figure 4.

Another interesting observation was the elutriation of particles at much lower superficial velocities. This is attributed to the formation of channels in the bed: for a given superficial velocity, the air velocity within these channels or crevices can be high enough to cause localised elutriation of loose particles. This loss of particles may also hinder the applicability of fluidisation of nanoparticle agglomerates in industrial processes.

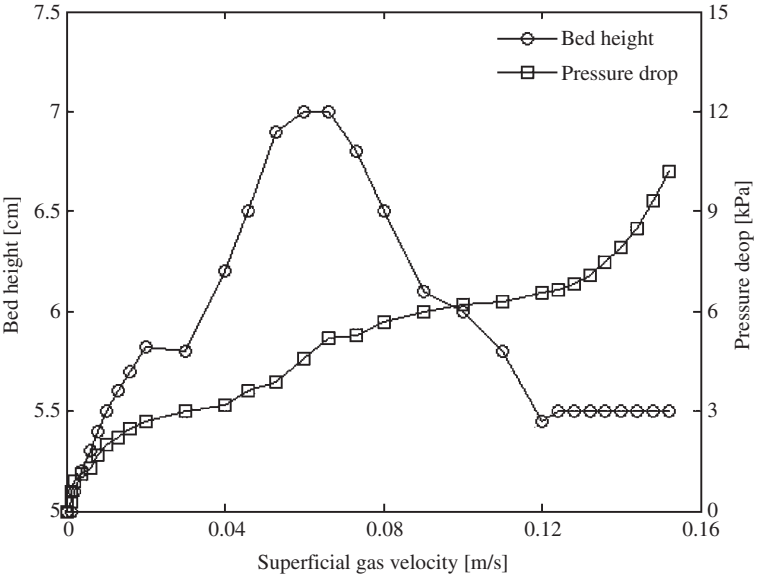

Figure 3. Typical pressure drop and bed height curves for unassisted ($f = 0$ Hz) fluidisation of silica nanoparticles (Aerosil 300).

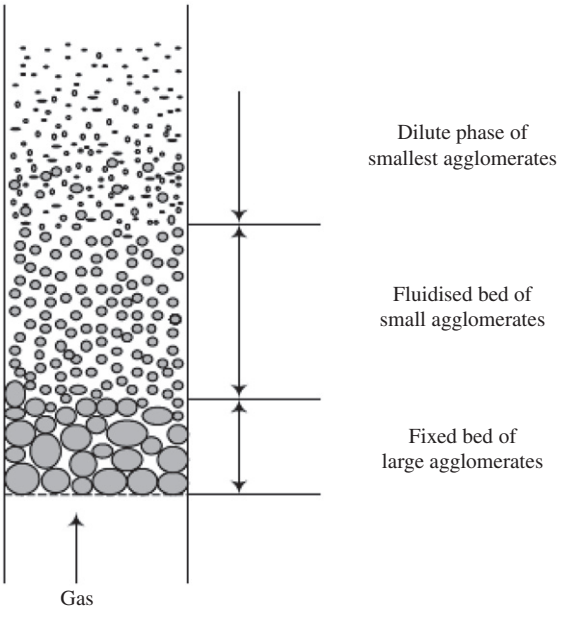

Figure 4. The conceptual model of Li et al. [18] illustrates the axial stratification of particles into agglomerates layers of different sizes.

3.2. *Fluidisation characteristics under mechanical vibration*

As discussed earlier, the problems associated with fluidising Geldart Group C particles led several researchers to investigate the use of mechanical agitation to achieve smooth fluidisation. As reported by Nam and Pfeffer [19], in these studies mechanical agitation was found to improve the fluidisation of micron sized Geldart C cohesive particles, eliminating the channelling, 'rat-hole' and plugging often associated with these materials. In their work, Nam et al. used a similar system to that employed here to study silica nanoparticles, but with the vertical vibration and its frequencies between 30 and 200 Hz, and using an acrylic column rather than glass. We suspect that the use of a plastic column will cause uncertainty in the measurement due to the build-up static electricity.

In Section 3.1, we demonstrated that in the absence of vibration, the bed exhibited typical Geldart C behaviour, i.e. cracking channelling, and 'rat holing', coupled with the formation of a packed bed of large agglomerates located adjacent to the distributor, which is shown conceptually in Figure 5(a)–(c). Under the assistance of vibration, stable channels formed by the cohesive forces were eliminated and the fluidisation state was significantly improved (Figure 5d). Typical fluidisation curves, showing bed expansion versus superficial gas velocity and illustrating the influence of vibration on the fluidisation behaviour of the silica nanoparticles are shown in Figure 6. Generally speaking, as the frequency of vibration increased, bed expansion also increased, irrespective of particle type. Nevertheless, we were unable to achieve smooth fluidisation with high bed expansion

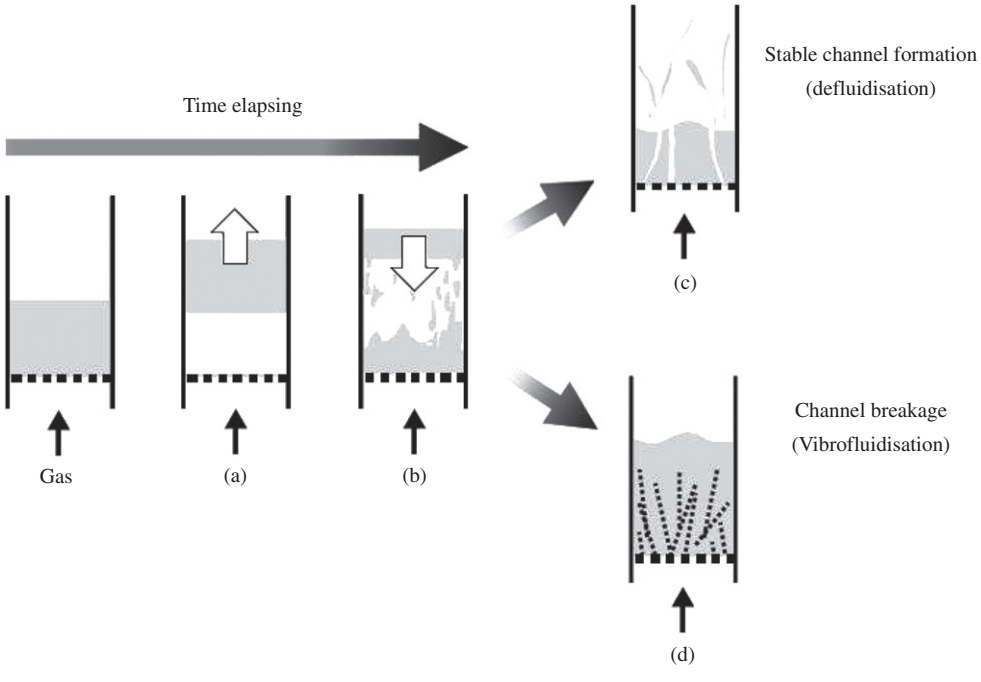

Figure 5. Schematic comparison of bed flow patterns between conventional and vibrofluidised bed.

(APF, using the terminology of Wang et al.) in all cases, at the frequencies above 8.7 Hz. We were able to fluidise all types of silica nanoparticles tested, at the frequencies considerably lower than previous reported, while the vibration intensity was set necessarily above 1 in all cases. This indicates that vibration intensity is a more deciding factor in the performance of vibrofluidised bed. In the case of the Aerosil 300 particle, which is hydrophilic, at 8.7 Hz, bed expansion was achieved at much higher superficial gas velocities than for the other particle, including Aerosil R812 which has the same particle size and density as Aerosil 300. This suggests that moisture in the atmosphere is sufficient to significantly affect the fluidisation of this material.

In Figure 7, the evolution of bed height versus superficial gas velocity as a function of particle type and vibration parameters is shown. There are three important observations from this data:

(i) R812 has the highest bed expansion of all the three particles at any of the vibration intensities studied,
(ii) the optimum frequency for maximising bed expansion is in the region of 25 Hz for all the three particles and
(iii) Aerosil 300 appeared not to benefit from fluidisation at higher frequencies, instead transforming to an agglomerate bubbling system, although this may be due to external forces not measured during the experiment, e.g. atmospheric moisture content.

3.3. *Hysteresis effect*

Previous investigations of Geldart A, B and C particle fluidisations observed a hysteresis in the bed expansion behaviour during fluidisation and defluidisation cycles [20,21]. This is believed to be caused by the existence of yield stresses caused, for example, by friction due to particles contact with the walls of the column [22,23], which reportedly resulted in plugging or channelling of the nanoparticle agglomerates at low velocities. Similarly, in this work, typical hysteresis effects to different degrees were observed in the bed expansion measurement for all three types of silica nanoparticles. Of these, Aerosil 300, the only hydrophilic particle studied, is most pronounced in the hysteresis curves obtained. This is shown in Figure 8, and indicates the influence of the humidity on yield stresses in the bed. We also noted that hysteresis effects for nanoparticles studied in this work were most pronounced in the absence of mechanical agitation, or at very low vibration frequencies ($<$16.7 Hz), irrespective of the particle type. At the frequencies greater than this, hysteresis effects were still evident, but were considerably less pronounced.

3.4. *Bed collapse experiments*

The bed collapse technique, first reported by Rietema in 1967, is one of the standard techniques widely used to study hydrodynamic properties of fines or more generally for particles belonging to group A of Geldart classification [24]. According to previous works, in the absence of mechanical vibration, the bed collapse process of Geldart A and C particles was established into three distinct, consecutive stages: (1) the bubbles escape, (2) hindered sedimentation and (3) the solid consolidation [18]. For three types of silica

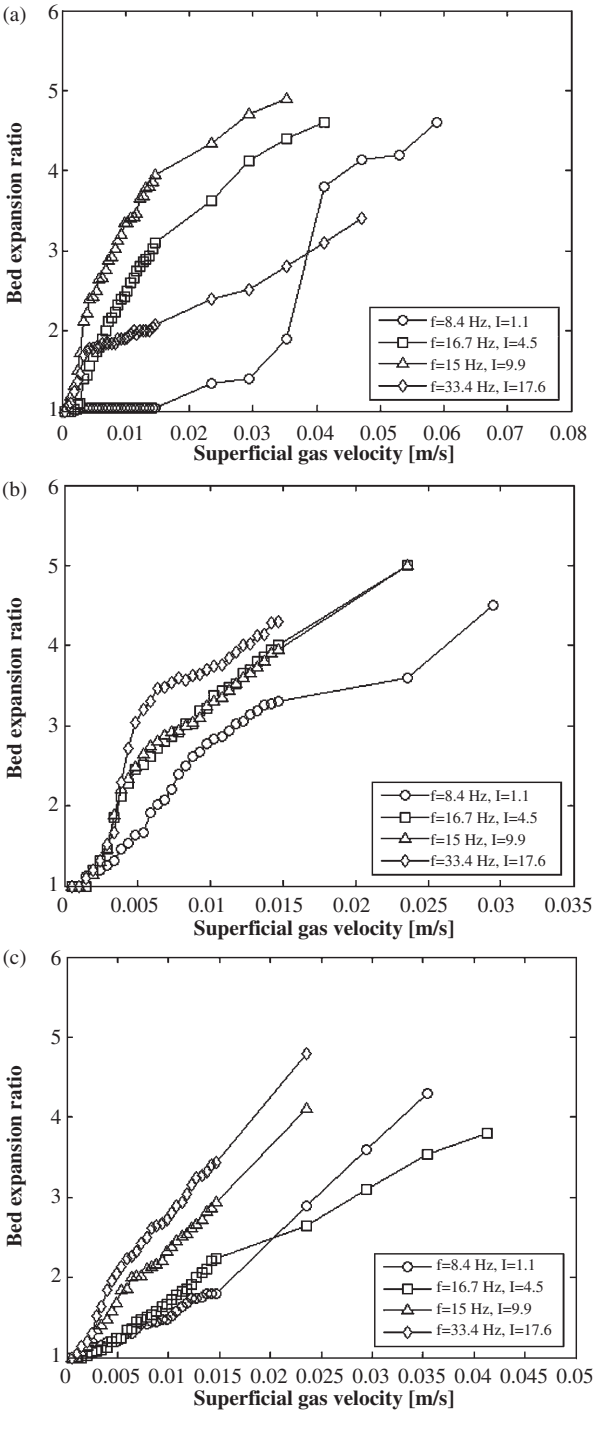

Figure 6. Bed expansion versus superficial gas velocity as a function of vibration parameters (frequency and intensity) for (a) Aerosil 300; (b) Aerosil R812 and (c) Aerosil R972.

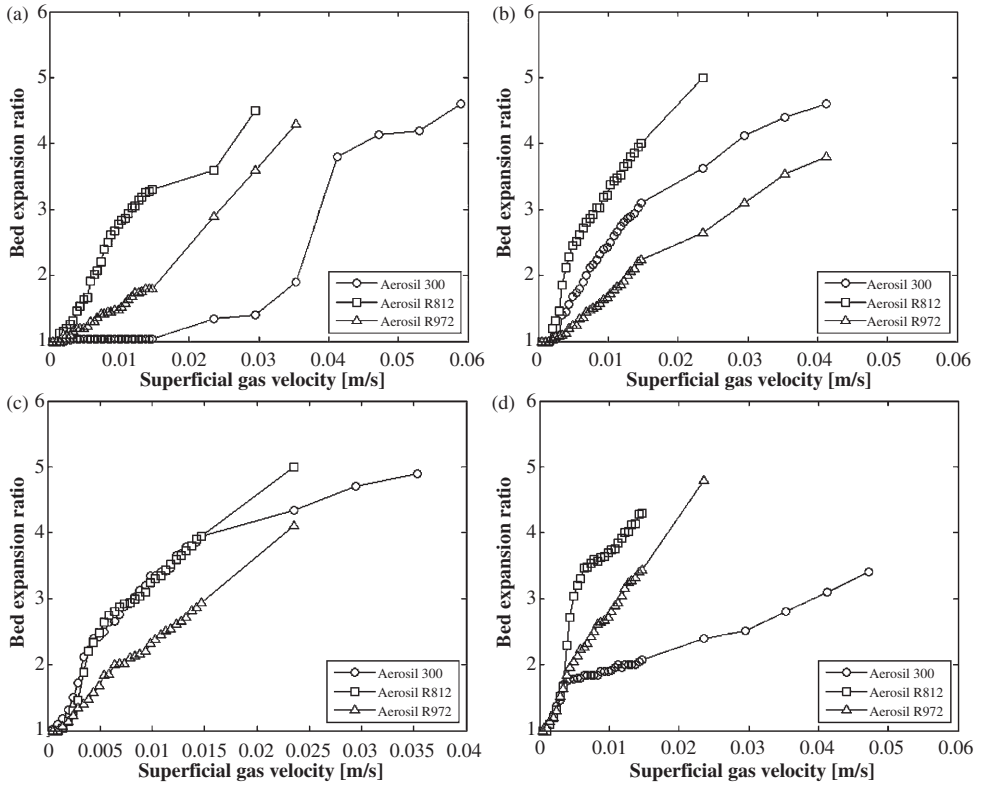

Figure 7. Evolution of bed height versus superficial gas velocity as a function of particle type and vibration parameters: (a) $f = 8.4$ Hz, $I = 1.1$; (b) $f = 16.8$ Hz, $I = 4.5$; (c) $f = 25$ Hz, $I = 9.9$ and d) $f = 3.4$ Hz, $I = 19.6$.

nanoparticles studied in this work, we observed similar bed collapse behaviours, in both cases with and without the vibration presence:

(i) In the first stage, the surface fluctuates due to the gas bubbles reaching the top of the bed and bursting.
(ii) In the second stage, with the fall of the bed height, the top section is still fluidised while the bottom has settled to a fixed bed and the interface between these two sections is moving upwards while bed surface is collapsing.
(iii) In the third stage, the top of the settling zone reached the fixed bed layer at the bottom, and a slow compaction of the particles begun depending on the particle characteristics.

Accordingly, typical bed collapsing curves as a function of time were generated in Figure 9, in which the aforementioned bed collapse stages are reflected on three segments, a sharp falling section (stage one) followed by a slower, nearly linear decline (stage two) and plateau (stage three). In addition, another type of bed collapsing curve, which features the settling of fully expanded bed without the vibration presence but aeration, was also obtained. The bed collapse curve of this type, interestingly shows some

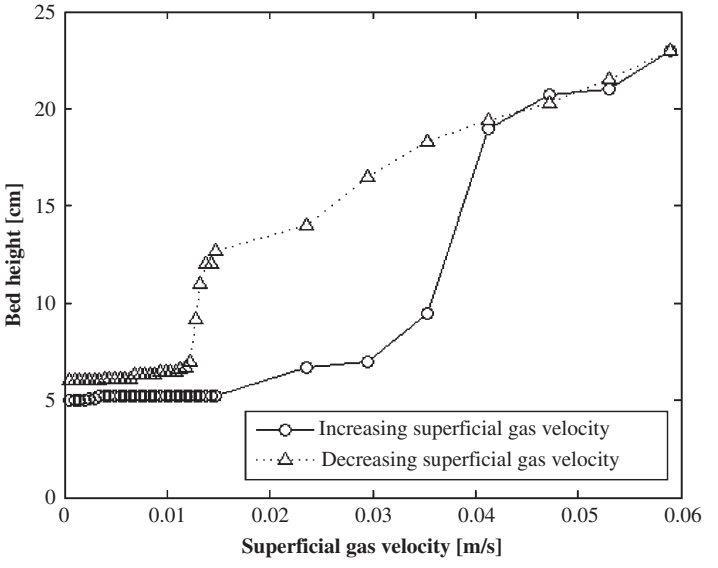

Figure 8. Bed height versus superficial gas velocity for sequential measurements showing hysteresis loops in the bed height profiles for Aerosil 300. The difference in the bed height at the same superficial gas velocity between the fluidisation and defluidisation cycle is most likely due to the condensation of bed particles into discrete agglomerates.

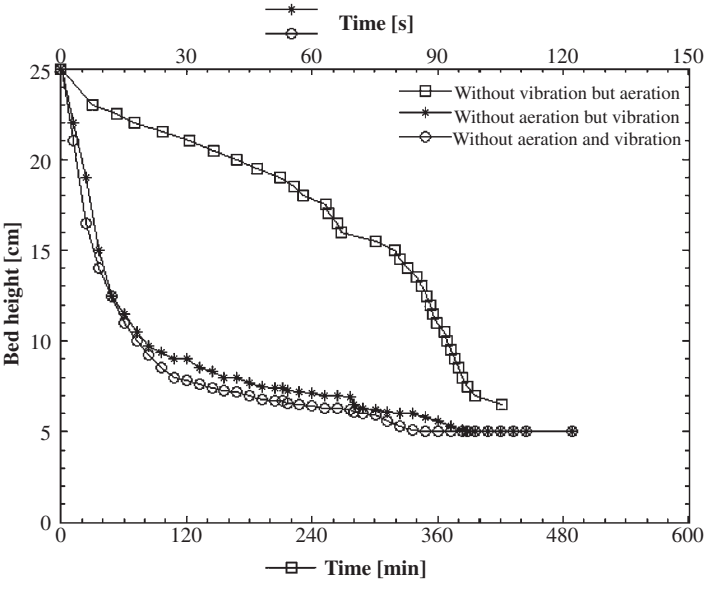

Figure 9. A typical bed collapse behaviour of Aerosil R812 with vibration at $f = 33.4$ Hz.

discrepancies, and by comparison several important observations can be derived from Figure 9:

(i) Without aeration, the bed collapsed to its initial height within 2 min for all three types of silica nanoparticles, irrespective of the vibration presence.
(ii) The presence of vibration did appear to slow the settling rate, however, its influence was very limited.
(iii) Once the bed was fluidised with the aid of vibration and aeration, the aeration alone was sufficient to sustain the bed in a fluidised and expanded state for a considerable amount of time (~10 h) even after the mechanical vibration was abruptly switched off.

Based on similar observations, among the first, Nam et al. postulated that once the bed was fluidised under the mechanical vibration, the original inter-particle networks caused by cohesive forces were disrupted, and the resulting agglomerates did not form strong cohesive networks, which was detrimental to successful fluidisation [19]. This also suggested an existence of favourable agglomerate sizes for fluidisation, which was balanced between the mechanical vibration-induced breaking and cohesive forces-induced forming. When the vibration was turned off, it took time for this balance to shift back to the unfavourable fluidisation state (the point at which the bed began to collapse). In addition, we found that the prolonged settling time is influenced by the particle and fluid properties. For example, we noted that among three types of silica nanoparticles, Aerosil 300 appeared to be the one with the shortest settling time under the same experimental conditions. This is probably due to their hydrophilic surface property, which could enhance cohesive forces in the presence of humidity.

4. Conclusions

This study has shown that three types of silica nanoparticles (Aerosil 300, R812 and R972) with primary particle sizes between 7 and 16 nm are very difficult to fluidise in the absence of external agitation. With the assistance of mechanical vibration, stable channels formed by the cohesive forces were eliminated, and the fluidisation state was significantly improved. Horizontal vibration was proved to be as effective as the vertical configurations reported previously. Bed expansion (a measure of fluidisation quality) increased significantly with increasing vibration rate. However, once the fluidisation of nanoparticles was achieved, it played little role on the bed collapse process. Furthermore, our results show that silica nanoparticles can be fluidised uniformly at vibration frequencies lower than in previous studies, as long as the vibration intensity was necessarily kept above 1. Consequently, we conclude that the use of low-frequency external agitation is an effective aid in improving the quality of fluidisation for nanoparticle material. Further research with a wider range of nanoparticle materials is needed to correlate nanoparticle properties with the fluidisation behaviour.

Acknowledgements

Authors are indebted to Dr Andrew Harris for his assistance in preparing the manuscript of this article and Degussa AG for supplying us with the silica nanoparticles.

References

[1] O. Molerus, *Interpretation of Geldart's type A, B, C and D powders by taking into account interparticle cohesion forces*, Powder Technol. 33 (1982), pp. 81–87.
[2] D. Geldart, *Type of gas fluidization*, Powder Technol. 7 (1973), pp. 285–292.
[3] F.E. Kruis, H. Fissan, and A. Peled, *Synthesis of nanoparticles in the gas phase for electronic, optical and magnetic applications – A review*, J. Aerosol Sci. 29 (1998), pp. 511–535.
[4] M.N. Rittner, *Market analysis of nanostructured materials*, Am. Ceram. Soc. Bull. 81 (2002), pp. 33–36.
[5] N. Ichinose, Y. Ozaki, and S. Kashu, *Superfine Particle Technology*, Springer-Verlag, London, 1992.
[6] W. Zhang, *A review of techniques for the process intensification of fluidized bed reactors*, Chin. J. Chem. Eng. 4 (2009), pp. 688–702.
[7] A. Dutta and L.V. Dullea, *Effects of external vibration and the addition of fibers on the fluidization of a fine powder*, AIChE Symp. Ser. 87 (1991), pp. 38–46.
[8] E. Jaraiz, S. Kimura, and O. Levenspiel, *Vibrating beds of fine particles: Estimation of interparticles forces from expansion and pressure drop experiments*, Powder Technol. 72 (1992), pp. 23–30.
[9] E. Marring, A.C. Hoffman, and L.P.B.M. Janssen, *The effect of vibration on the fluidization behaviour of some cohesive powders*, Powder Technol. 79 (1992), pp. 1–10.
[10] Y. Mawatari, T. Koide, Y. Tatemoto, S. Uchida, and K. Noda, *Effect of particle diameter on fluidization under vibration*, Powder Technol. 123 (2002), pp. 69–74.
[11] S. Mori, A. Yamamoto, S. Iwata, T. Haruta, and I. Yamada, *Vibrofluidization of Group-C particles and its industrial applications*, AIChE Symp. Ser. 86 (1990), pp. 88–94.
[12] S.M. Tasirin and N. Anuar, *Fluidization behaviour of vibrated and aerated beds of starch powders*, J. Chem. Eng. Jpn 34 (2001), pp. 1251–1258.
[13] J.R. Wank, S.M. George, and A.W. Weimer, *Vibro-fluidization of fine boron nitride powders*, Powder Technol. 121 (2001), pp. 195–204.
[14] K. Erdesz, *Hydrodynamic aspects of conventional and vibrofluidized beds – A comparative evaluation*, Powder Technol. 46 (1986), pp. 167–172.
[15] J.M. Valverde, *Effect of vibration on the stability of a gas-fluidized bed of fine powder*, Phys. Rev., E. Stat. Phys. Plasmas Fluids Relat. Interdiscip. Topics 64 (2001), p. 21302.
[16] Y. Wang, G. Gu, F. Wei, and J. Wu, *Fluidisation and agglomerate structure of SiO_2 nanoparticles*, Powder Technol. 124 (2002), pp. 152–159.
[17] C. Zhu, Q. Yu, R.N. Dave, and R. Pfeffer, *Gas fluidization characteristics of nanoparticle agglomerates*, AIChE J. 51 (2005), pp. 426–439.
[18] H. Li, X. Lu, and M. Kwauk, *Particulatization of gas–solids fluidization*, Powder Technol. 137 (2003), pp. 54–62.
[19] C.H. Nam, R. Pfeffer, R.N. Dave, and S. Sundaresan, *Aerated vibrofluidization of silica nanoparticles*, AIChE J. 50 (2004), pp. 1776–1785.
[20] J. Heck and U. Onken, *Hysteresis effects in suspended solid particles in bubble columns with and without a draft tube*, Chem. Eng. Sci. 42 (1987), pp. 1211–1212.
[21] D. Petrovic, D. Posarac, and D. Skala, *Hysteresis effects of minimum fluidization velocity in a draft tube airlift reactor*, Chem. Eng. Sci. 44 (1989), pp. 996–998.
[22] P.N. Loezos, P. Costamgna, and S. Sundaresan, *The role of contact stresses and wall friction on the fluidization*, Chem. Eng. Sci. 57 (2002), pp. 5123–5141.
[23] S.C. Tsinontides and R. Jackson, *The mechanics of gas fluidised beds with an interval of stable fluidization*, J. Fluid Mech. 225 (1993), pp. 237–274.
[24] K. Rietema, Application of mechanical stress theory to fluidization. Proceedings of the International Symposium on Fluidization, Toulouse, 1967, p.157.